

Supplemental Figure Legends

Figure S1. Repression of *rrs* Transcription by the PhoP-Activated *mgtA*, *mgtB* and *mgtC* Genes, Related to Figures 2 and 3.

(A) *rrs* transcriptional activity of wild-type *Salmonella* (14028s) grown in high (10 mM), and wild-type (14028s) and *phoP* (MS7953) *Salmonella* grown in low (10 μ M) Mg^{2+} . Error bars represent standard deviations.

Graph is the average of three independent qPCR experiments. (B) % of *rrs* leader rRNA region in wild-type (14028s) and *phoP* (MS7953) *Salmonella* following rifampicin (200 μ g/ml) treatment to stop new transcription. Error bars represent standard deviations.

Graph is the average of four independent experiments. (C) Electrophoretic mobility shift assays of DNA fragments harboring the *Salmonella phoP*, *hisL*, *rrsC* P1 and *rrsC* P2 promoters with phosphorylated PhoP protein. The gel is representative of three independent experiments.

(D) Primer extension analyses of wild-type (14028s), *mgtC* (EL4) and *mgtC* (EL4) *Salmonella* harboring the *mgtC*-expressing plasmid (pMgtC) or the plasmid vector (pUHE-21-2-*lacI^q*) following growth in low Mg^{2+} .

(E) Primer extension analyses of wild-type (14028s), *mgtA mgtB* (EG16741) and *mgtA mgtB* (EG16741)

Salmonella harboring the *mgtA*-expressing plasmid (pMgtA) or the plasmid vector

(pUHE-21-2-*lacI^q*) during growth in low Mg^{2+} .

(F) Primer extension analyses of wild-type (14028s), *phoP* (MS7953) and *phoP* (MS7953) *Salmonella* harboring the plasmid vector (pUHE-21-2-*lacI^q*), the *mgtB*-expressing plasmid (pMgtB), pMgtC and the *mgtCB*-expressing plasmid (pMgtCB). For *rrs* primer extension: lanes 1 and 2, and 3 to 5

correspond to lanes 1 and 2, and 9 to 12 of the gel displayed on Figure S7C, respectively.

(G) ATP levels of wild-type (14028s), *mgtA mgtB* (EG16741), *mgtC* (EL4), *mgtA mgtB mgtC* (EG16738) and *phoP* (MS7953) *Salmonella* strains following 6 h growth in low Mg^{2+} .

All measurements were carried following 6 h growth in low Mg^{2+} N-minimal medium ($OD_{600} \approx 0.4-0.6$). Primer extension analyses are representative of 2-4 independent experiments.

Figure S2. The PhoP-Activated *mgtA*, *mgtB* and *mgtC* Genes Repress *rrs* P1 Promoters, Related to Figures 2 and 3. (A) *gfp* mRNA levels in wild-type (14028s), *mgtC* (EL4) and *mgtA mgtB* (EG16741) *Salmonella* harboring pP1_{*rrsC*}-*gfp*_{AAV} following 6 h growth in low (10 μ M) Mg^{2+} N-minimal medium ($OD_{600} \approx 0.4-0.6$). Error bars represent standard deviations. Graphs show the average of four independent experiments analyzed by qPCR. Values are normalized to those of the constitutively transcribed *bla* gene, which is also in the plasmid. (B) Schematic illustration of plasmid pP1_{*rrsC*}-*gfp*_{AAV} , containing a transcriptional fusion between *Salmonella*'s *rrsC* P1 promoter and an unstable *gfp* reporter gene. (C) Sequence alignment of *Salmonella rrs* P1 promoters. Promoters' UP-element is underlined, -35 and -10 regions are in bold and highlighted in gray, and transcription start site (+1) is depicted in red.

Figure S3. Effects of Mg^{2+} Starvation on Growth, ATP and ppGpp Levels, Related to Figure 3. (A) Detection of ^{32}P -labeled ppGpp by thin layer chromatography (TLC). Leftmost: ^{32}P -labeled nucleotides derived from wild-type (14028s) (positive control) and *relA spoT* (MP342) (negative control) *Salmonella* following 30 min treatment with serine hydroxamate (Shx, 50 μ g/ml). Rightmost: nucleotides derived from wild-type (14028s), *mgtC* (EL4) and *mgtC* (EL4) *Salmonella* harboring the *mgtC*-expressing plasmid (pMgtC) or the plasmid vector (pUHE-21-2-*lacI*^q). Nucleotides were extracted following 6 h of growth in low (10 μ M) Mg^{2+} MOPS (leftmost strains) or N-minimal medium (rightmost

strains) ($OD_{600} \approx 0.4-0.6$). Arrows indicate signals corresponding to ATP, GTP, ppGpp and the origin. Top TLC shows signals from the origin to ATP. Bottom TLC shows high-contrasted region encompassing the origin to GTP. TLCs are representative of four independent experiments. (B) Quantification of ATP levels in wild-type (14028s) and *mgtC* (EL4), and *relA spoT* (MP342) and *mgtC relA spoT* (MP343) *Salmonella* following 6 h growth in MOPS glucose medium containing low Mg^{2+} . Error bars represent standard deviations. Graphs show the average of four independent experiments. (C) Growth curves of wild-type (14028s), *mgtC* (EL4), *relA spoT* (MP342) and *mgtC relA spoT* (MP343) *Salmonella* in MOPS glucose medium containing low (10 μM) Mg^{2+} . Dashed lines indicate the time where wild-type (14028s) and *mgtC* (EL4), and *relA spoT* (MP342) and *mgtC relA spoT* (MP343) *Salmonella* experience cytosolic Mg^{2+} starvation.

Figure S4. MgtA and MgtB Maintain Cytosolic Mg^{2+} Concentrations, Related to Figures 2 and 6. (A) Cartoon representation of the genetic reporter for cytosolic Mg^{2+} levels present in the $pP_{lac1-6}-mgtA_{leader}-lacZ$ plasmid. This reporter consists of a constitutive promoter driving transcription of *Salmonella's mgtA* Mg^{2+} -sensing riboswitch fused to a promoterless *lacZ* gene. When cytosolic Mg^{2+} levels decrease, the riboswitch adopts a conformation that allows transcription to continue into *lacZ*, resulting in heightened β -galactosidase activity (Cromie et al., 2006). (B) Cartoon representation of the control $pP_{lac1-6t}-lacZ$, consisting of an isogenic *lacZ* fusion lacking the Mg^{2+} -sensing riboswitch (Cromie et al., 2006). β -galactosidase activities derived from this control fusion can serve as normalization factor, by accounting for potential differences in p_{lac1-6} promoter activity or *lacZ* translation efficiency across strains. (C) β -

galactosidase activities of wild-type (14028s), *mgtA mgtB* (EG17048) and *mgtA mgtB* (EG17048) *Salmonella* harboring the *mgtA*-expressing plasmid (pMgtA), the *mgtB*-expressing plasmid (pMgtB) or the plasmid vector (pUHE-21-2-*lacI^q*) with pP_{*lacI-6*}-*mgtA*_{leader}-*lacZ* or pP_{*lacI-6r*}-*lacZ* in following 6 h growth in low (10 μ M) Mg²⁺ N-minimal medium (OD₆₀₀ \approx 0.4-0.6).

Figure S5. MgtA, MgtB and MgtC Enable Translation During Cytosolic Mg²⁺

Starvation, Related to Figure 4. (A) Leftmost panel: Polysome analysis of wild-type (14028s) *Salmonella* after 3 h growth in high (10 mM) Mg²⁺ N-minimal medium (OD₆₀₀ \approx 0.5-0.6). Rightmost panel: denaturing agarose gel electrophoretic analysis of polysomal fractions shown on the leftmost panel. Polysome profile is representative of four independent experiments. (B) SDS-PAGE analysis of L-azidohomoalanine (AHA) labeling of wild-type (14028s), *mgtC* (EL4) and *mgtC* (EL4) *Salmonella* harboring the *mgtC*-expressing plasmid (pMgtC) or the plasmid vector (pUHE-21-2-*lacI^q*) during growth in low (10 μ M) Mg²⁺. (C) SDS-PAGE analysis of AHA labeling of wild-type (14028s), *mgtA mgtB* (EG16741) and *mgtA mgtB* (EG16741) *Salmonella* harboring the *mgtA*-expressing plasmid (pMgtA) or the plasmid vector (pUHE-21-2-*lacI^q*) during growth in low Mg²⁺. In (B) and (C), bacteria were grown in low (10 μ M) Mg²⁺ N-minimal medium lacking methionine. AHA labeling was carried out from 5.5 to 6 h growth (final OD₆₀₀ \approx 0.4-0.5). Gels are representative of four independent experiments.

Figure S6. MgtA and MgtB Promote Translation by Importing Mg²⁺, Whereas MgtC

Enables Translation by Redistributing Cytosolic Mg²⁺, Related to Figure 4. (A)

Quantification and SDS-PAGE analysis of L-azidohomoalanine (AHA) labeling of wild-

type (14028s) and *mgtC* (EL4) *Salmonella* harboring the ATPase expressing plasmid pATPase or the plasmid vector (pCP44) during growth in low (10 μ M) Mg^{2+} . (B) Quantification and SDS-PAGE analysis of AHA labeling of wild-type (14028s) and *mgtC* (EL4) strains of *Salmonella* harboring the *mgtA*-expressing plasmid (pMgtA) or the plasmid vector (pUHE-21-2-*lacIⁿ*) during growth in low Mg^{2+} . (C) Quantification and SDS-PAGE analysis of AHA labeling of wild-type (14028s) and *mgtA mgtB* (EG16741) *Salmonella* harboring pATPase or the plasmid vector (pCP44) during growth in low Mg^{2+} . Strains were grown in low Mg^{2+} N-minimal medium lacking methionine. AHA labeling was carried out from 5.5 to 6 h growth (final $OD_{600} \approx 0.4-0.5$). Error bars represent standard deviations. Graphs show the average of four independent experiments. Gels are representative of four independent experiments.

Figure S7. Ribosomal *rrs* primer extension analyses, Related to Figure 3. (A) Primer extension analyses of wild-type (14028s; lane 1), *mgtC* (EL4; lane 2), and *mgtC* (EL4) *Salmonella* harboring the ATPase expressing plasmid pATPase (lane 7) or the plasmid vector (pCP44; lane 8) during growth in low (10 μ M) Mg^{2+} . (B) Primer extension analyses of wild-type (14028s; lane 1), *mgtC* (EL4; lane 2), *relA spoT* (MP342; lane 5) and *mgtC relA spoT* (MP343; lane 6) *Salmonella* growth in MOPS glucose medium containing low (10 μ M) Mg^{2+} . (C) Primer extension analyses of wild-type (14028s; lane 1), *phoP* (MS7953; lane 2) and *phoP* (MS7953) *Salmonella* harboring the plasmid vector (pUHE-21-2-*lacIⁿ*; lane 9), the *mgtB*-expressing plasmid (pMgtB; lane 10), pMgtC (lane 11) and the *mgtCB*-expressing plasmid (pMgtCB; lane 12).

Supplemental Tables

Table S1. Bacterial Strains and Plasmids Used in this Study, Related to Figures 2, 3, 4 and 5.

Table S2. Oligonucleotides Sequences Used in this Study, Related to Figures 2, 3, 4 and 5.

Supplemental Experimental Procedures

Construction of *mgtC rpoB*_{L533P} and *mgtC rpoB*_{A532A} Strains. Introduction of point mutations in the *rpoB* gene was carried out via λ -red-mediated recombination (Datsenko and Wanner, 2002), by integrating synthetic double stranded oligonucleotides containing the desired mutations into the chromosome of wild-type *Salmonella* and selecting recombinants on LB plates containing 50 $\mu\text{g}/\text{mL}$ of rifampicin. As rifampicin resistant (Rif^{R}) colonies emerge at relatively high frequency, the identification of the correct mutations was accomplished by screening Rif^{R} clones by PCR and DNA sequencing. Correct *rpoB* alleles were moved into *mgtC* (EL4) mutant strain of *Salmonella* via P22-mediated transduction (Davis et al., 1980). Screening Rif^{R} colonies by PCR and DNA sequencing identified the correct clones.

L-azidohomoalanine (AHA) Labeling and Quantification. *Salmonella* strains were grown overnight in N-minimal medium containing high Mg^{2+} . Overnight cultures were washed 3x in N-minimal medium lacking Mg^{2+} and casamino acids, and inoculated 1:25

(strains harboring pATPase plasmid) or 1:50 (all other strains) in low Mg^{2+} N-minimal containing an amino acids mixture lacking methionine (Mix_{-Met}: 1.6 mM of alanine, glycine, leucine, glutamate and serine, 1.2 mM glutamine and isoleucine, 0.8 mM arginine, asparagine, aspartate, lysine, phenylalanine, proline, threonine and valine, 0.4 mM histidine and tyrosine, and 0.2 mM cysteine and tryptophan). Following 2.5 or 5.5 h of growth, cultures were labeled with 40 μ M of AHA for 30 min (Click Chemistry Tools).

E. coli strains were grown overnight in high Mg^{2+} MOPS medium. The following day, cells were subcultured (1:100) into fresh high Mg^{2+} MOPS medium lacking casamino acids, but supplemented with Mix_{-Met}. Cultures were grown for 2 h, washed 3x and resuspended with the same medium lacking Mg^{2+} . Following 2 h, cultures were labeled with 400 μ M of AHA (Click Chemistry Tools) for 30 min. At the end of the labeling period, bacterial cultures were treated with chloramphenicol (100 μ g/ml). Cells were collected by centrifugation at 4°C, washed 3x with ice-cold phosphate buffered saline (PBS) and stored at -80°C.

Cell pellets were thawed and resuspended in a lysis buffer consisting of 50 mM Tris-HCl, pH 8.0, 0.5% sodium dodecyl sulfate (SDS) and 1x protease inhibitor cocktail (Roche). Cells were lysed by sonication and insoluble debris was removed by centrifugation (10 min, 10,000x rpms, 4°C). Covalent attachment of fluorescent tetramethylrhodamine (TAMRA)-alkyne (Thermo Fisher Scientific) to AHA containing proteins was carried out using Click-iT Protein Reaction Buffer Kit (Thermo Fisher Scientific) according to the manufacturer's instructions. Protein concentrations were determined using a Pierce BCA Protein Assay Kit (Thermo Fisher Scientific). Fluorescent signals in samples were measured in a Synergy H1 Reader (BioTek) with

545 nm excitation and 580 nm emission wavelengths. The rate of protein synthesis was estimated as the fluorescence signal normalized by the protein content of the sample.

To determine if alterations on protein synthesis were systemic, TAMRA-labeled samples were separated by SDS-PAGE and fluorescence in gels was captured with a Typhoon FLA 9000 (GE Healthcare Life Sciences) using a 532 nm excitation laser. To ensure that equal amounts of protein were loaded in each lane, gels were subsequently stained using the ProteoSilver Silver Stain Kit (Sigma-Aldrich).

Estimation of Cytosolic Mg²⁺. *Salmonella* strains harboring plasmid pP_{lac1-6}-*mgtA*_{leader}-*lacZ* or plasmid pP_{lac1-6}-*lacZ* (Cromie et al., 2006) were grown for in high Mg²⁺ N-minimal medium. Overnight cultures were washed 3x in Mg²⁺-free medium and inoculate (1:50) into fresh low Mg²⁺ N-minimal medium. Following 6 h of growth (OD₆₀₀ ≈ 0.4-0.6), β-galactosidase activities were determined as described (Cromie et al., 2006). *E. coli* cells harboring plasmid pP_{lac1-6}-*mgtA*_{leader}-*lacZ* or plasmid pP_{lac1-6}-*lacZ* (Cromie et al., 2006) were grown overnight in high Mg²⁺ MOPS medium. The next day, cells were subcultured (1:100) into fresh high Mg²⁺ MOPS medium and grown for 2.5 h. Cultures were then washed 3x with MOPS medium lacking Mg²⁺ and resuspended in the same medium or in high Mg²⁺ MOPS medium. β-galactosidase activities were then monitored through the course of 4 hours as described (Cromie et al., 2006). To account for differences in *plac*₁₋₆ promoter activity or translation efficiency across strains, β-galactosidase activity derived from pP_{lac1-6}-*lacZ* was used as an internal normalizing factor. Cytosolic Mg²⁺ concentrations were, therefore, derived from the following equation:

$$[\text{Mg}^{2+}] = 1 \div \left(\frac{(\text{Miller Units from pP}_{lac1-6}\text{-mgtA}_{leader}\text{-lacZ})}{(\text{Miller Units from pP}_{lac1-6}\text{-lacZ})} \right)$$

Electrophoretic mobility shift assay. DNA fragments corresponding to the *phoP*, *hisL*, *rrsC* P1 and *rrsC* P2 promoter regions were generated by PCR using wild-type *Salmonella* genomic DNA as template and primer pairs W2597 and W2598, W798 and W799, W2599 and W2600, W2601 and W2602, respectively. PCR products were separated on an 1.5% agarose gel and purified with QIAquick Gel Extraction Kit (Qiagen). 100 ng of DNA labeled with T4 polynucleotide kinase and [γ - 32 P]-ATP. Unincorporated [γ - 32 P]-ATP was removed by using G-50 microcolumns (GE Healthcare). 10 nmols of purified His-tagged PhoP* (Chamngopol and Groisman, 2000) was phosphorylated in PB buffer [20 mM Tris HCl pH 8.0, 2 mM MgCl₂, 180 mM KCl₂, 0.1 mM DTT and 40 mM acetyl-Pi] for 1 h at 37°C.

Approximately 10 fmols of labeled DNA probes were mixed with various amounts of PhoP-P in binding buffer [20 mM Tris HCl pH 8.0, 2 mM MgCl₂, 10 mM KCl₂, 10% (v/v) glycerol, 0.1 mM DTT, 60 μ g/mL BSA and 10 μ g/mL of poly (dI-dC)] in a total volume of 20 μ L. Following 20 min of incubation at room temperature, samples were electrophoresed on 4-20% Tris-borate-EDTA gels (Life Technologies) at 35 volts and 4°C.

Image Acquisition, Analysis and Manipulation. Fluorescence of TAMRA-labeled samples separated by SDS-PAGE was acquired with a Typhoon FLA 9000 (GE Healthcare Life Sciences) using a 532 nm excitation laser. 32 P signals from primer extension, nucleotide labeling or mobility-shift assays were acquired by exposing dried PEI-cellulose TLC or denaturing polyacrylamide gels to a phosphoscreen overnight. Signals from exposed phosphoscreens were acquired in a Typhoon FLA 9000 laser

scanner (GE Healthcare). For clarity, in images corresponding to certain *rrs* primer extension analyses, intervening samples were cropped out of the figures. The original, uncropped, figures are presented on Figure S7. In the images generated in the scan, the intensities of samples are often dimmed relative to high intensity portions of the image (e.g. the origin in the TLC or the excess primers in the primer extension analysis). Thus, the intensity of signals in the scanned images was adjusted across the entire images using the ImageJ software (Schneider et al., 2012). The intensity of particular bands was quantified using ImageJ (Schneider et al., 2012).

Supplemental References

Blattner, F.R., Plunkett, G.^{3rd}, Bloch, C.A., Perna, N.T., Burland, V., Riley, M., Collado-Vides, J., Glasner, J.D., Rode, C.K., Mayhew, G.F., et al. (1997). The complete genome sequence of *Escherichia coli* K-12. *Science* 277, 1453-1462.

Chamnongpol, S. and Groisman, E.A. (2002). Mg²⁺ homeostasis and avoidance of metal toxicity. *Mol. Microbiol.* 44, 561–571.

Choi, J., and Groisman, E.A. (2013). The lipopolysaccharide modification regulator PmrA limits *Salmonella* virulence by repressing the type three-secretion system Spi/Ssa. *Proc. Natl. Acad. Sci. USA.* 110, 9499-9504.

Cromie, M.J., Shi, Y., Latifi, T., and Groisman, E.A. (2006). An RNA sensor for intracellular Mg²⁺. *Cell* 125, 71-84.

Datsenko, K.A., and Wanner, B.L. (2000). One-step inactivation of chromosomal genes in *Escherichia coli* K-12 using PCR products. *Proc. Natl. Acad. Sci. USA.* 97,6640-6645.

Fields, P.I., Swanson, R.V., Haidaris, C.G., and Heffron, F. (1986). Mutants of *Salmonella typhimurium* that cannot survive within the macrophage are avirulent. Proc. Natl. Acad. Sci. USA. 83, 5189-5193.

Hanahan, D. (1985). Techniques for transformation of *E. coli*. In DNA Cloning: A Practical Approach, D.M. Glover, ed. (IRL Press, Oxford, United Kingdom), pp. 109 - 135.

Koebmann, B.J., Westerhoff, H.V., Snoep, J.L., Nilsson, D., and Jensen, P.R. (2002). The glycolytic flux in *Escherichia coli* is controlled by the demand for ATP. J. Bacteriol. 184, 3909-3916.

Lee, E.J., and Groisman, E.A. (2012). Control of a *Salmonella* virulence locus by an ATP-sensing leader messenger RNA. Nature 486, 271-275.

Lee, E.J., Pontes, M.H., and Groisman, E.A. (2013). A bacterial virulence protein promotes pathogenicity by inhibiting the bacterium's own F1Fo ATP synthase. Cell 154,146-156.

Park, S.Y., and Groisman, E.A. (2014). Signal-specific temporal response by the *Salmonella* PhoP/PhoQ regulatory system. Mol. Microbiol. 91, 135-144.

Schneider, C.A., Rasband, W.S., Eliceiri, K.W. (2012). NIH Image to ImageJ: 25 years of image analysis. Nature Methods 9, 671-675.

Sevostyanova, A., and Groisman, E.A. (2015). An RNA motif advances transcription by preventing Rho-dependent termination. Proc. Natl. Acad. Sci. USA. 112, E6835-E6843.

Soncini, F.C., Vescovi, E.G., Groisman, E.A. (1995). Transcriptional autoregulation of the *Salmonella typhimurium* *phoPQ* operon. J. Bacteriol. 177, 4364-4371.

Zwir, I., Shin, D., Kato, A., Nishino, K., Latifi, T., Solomon, F., Hare, J.M., Huang, H., and Groisman, E.A. (2005). Dissecting the PhoP regulatory network of *Escherichia coli* and *Salmonella enterica*. Proc. Natl. Acad. Sci. USA. 102, 2862-2867.

Figure S1

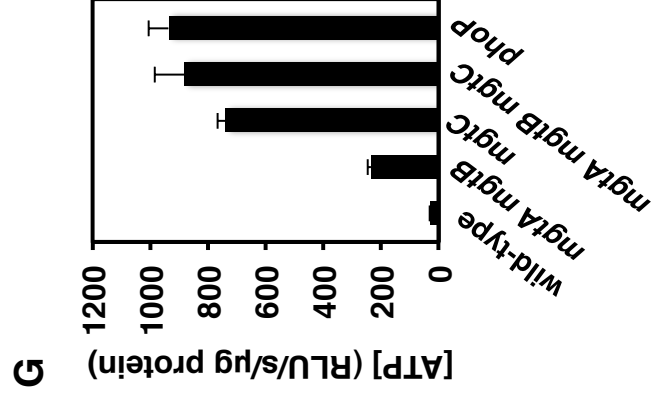
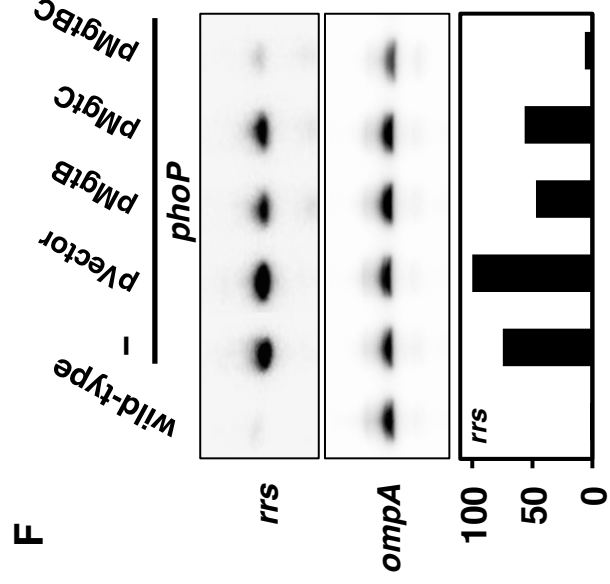
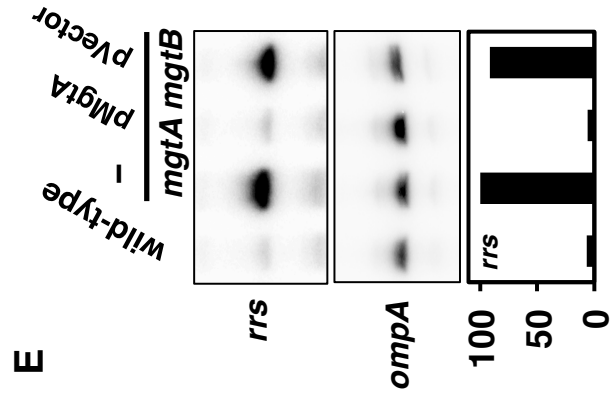
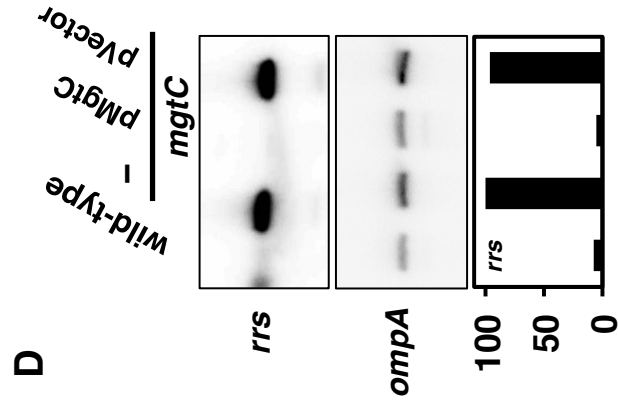
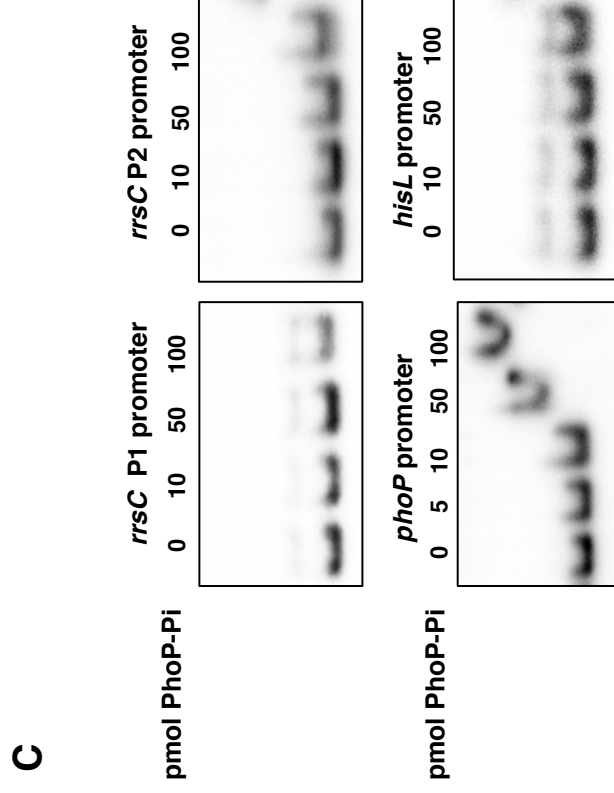
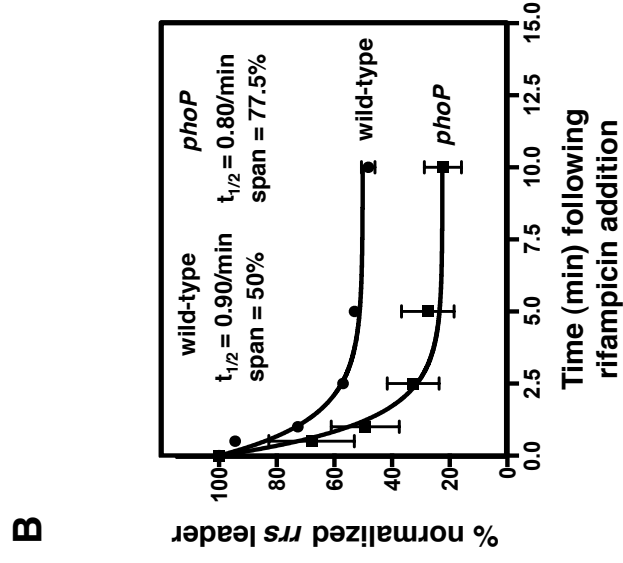
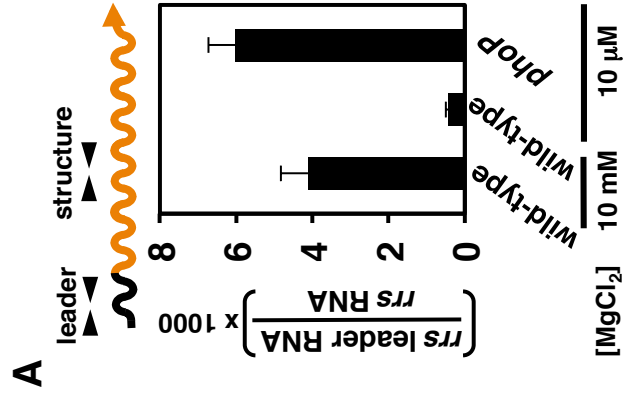
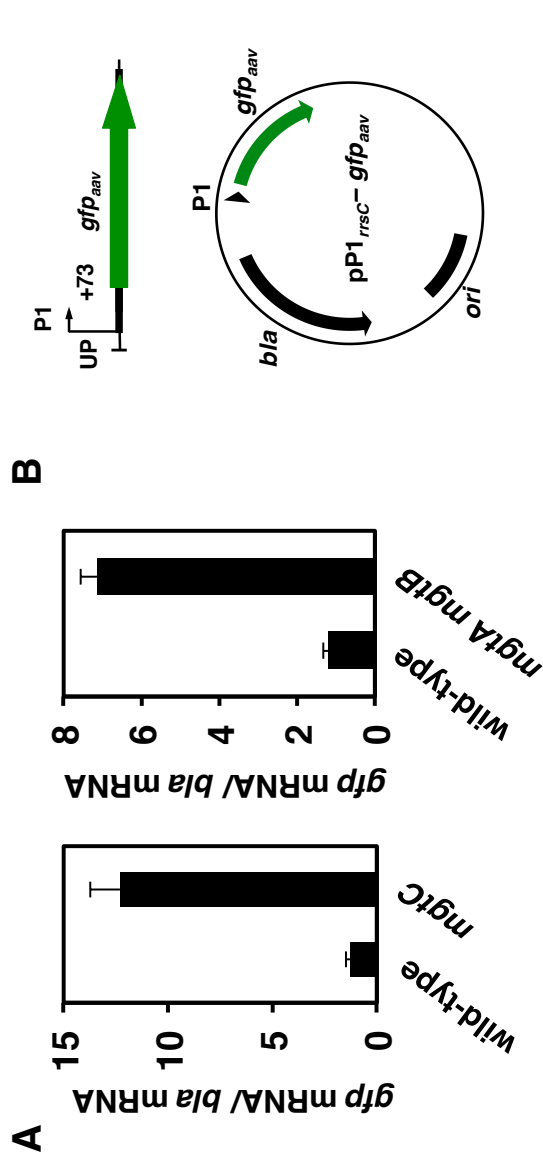


Figure S2



C

Salmonella enterica ribosomal P1 promoters

rrsA agaaaaattatttttaaaatttcctcttgtcaggcaaaaaataaactccctataataatgcccaccActgacacgggaacaa
rrsB gagaaaatttttaaaatttcctcttgtcaggcagaaaaataaactccctataataatgcccaccActgacacgggaacaa
rrsC agaaaaatttttaaaatttcctcttgtcaggcagaaaaataaactccctataataatgcccaccActgacacgggaacaa
rrsD agaaaaaaagatccaaaaaacgcttgtgcaaaaaaatgggatccctataataatgcccctccActgacacggcggat
rrsE gtcaatttctgcaattttctatgcggtcagcagagaactccctataataatgcccctccActgacacggcggat
rrsH aaaaacaaaaatgcatttttcccgccttgccttccctgaaccgactccctataataatgcccctccActgacacggcggat

UP-element -35 -10 +1

Figure S3

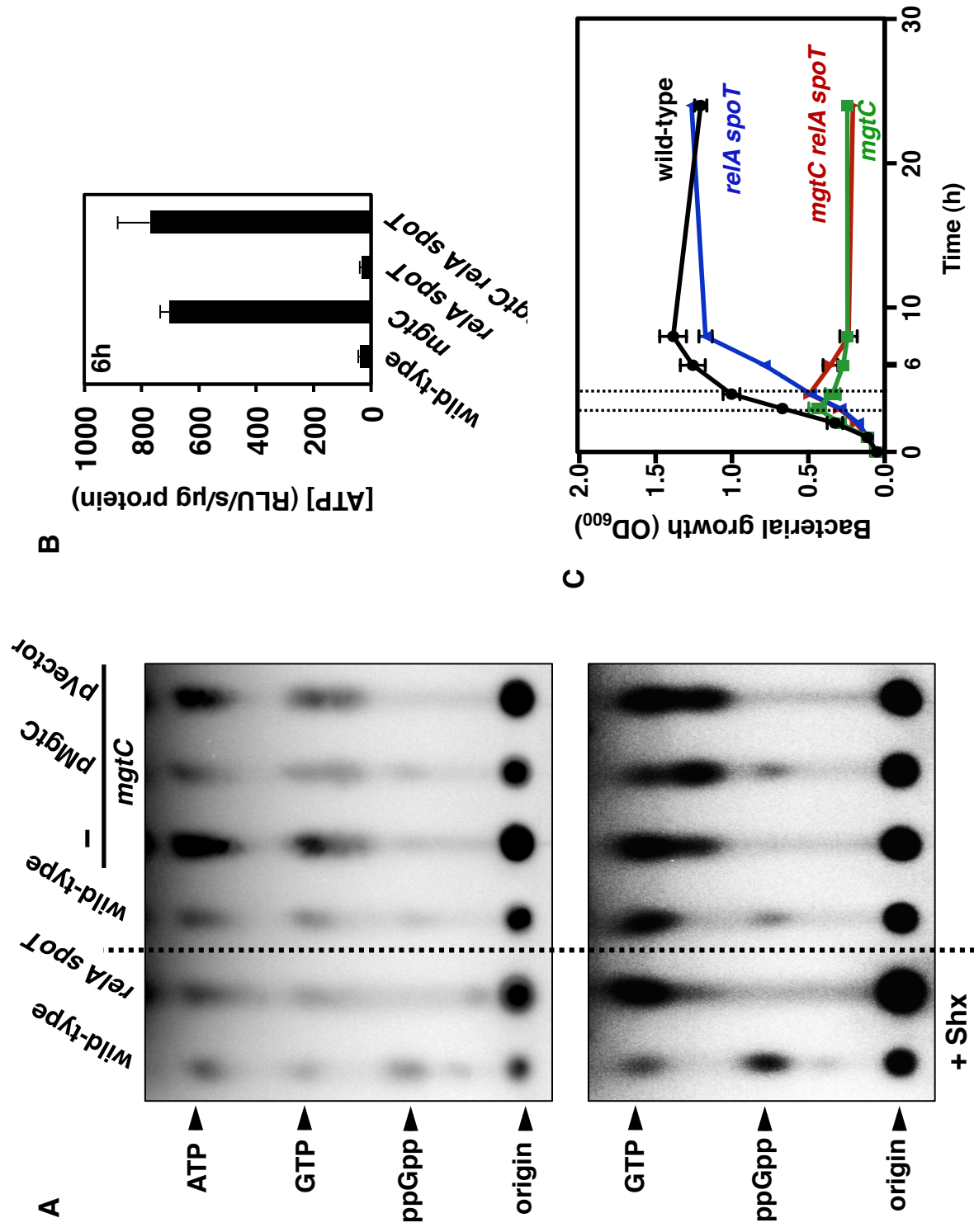


Figure S4

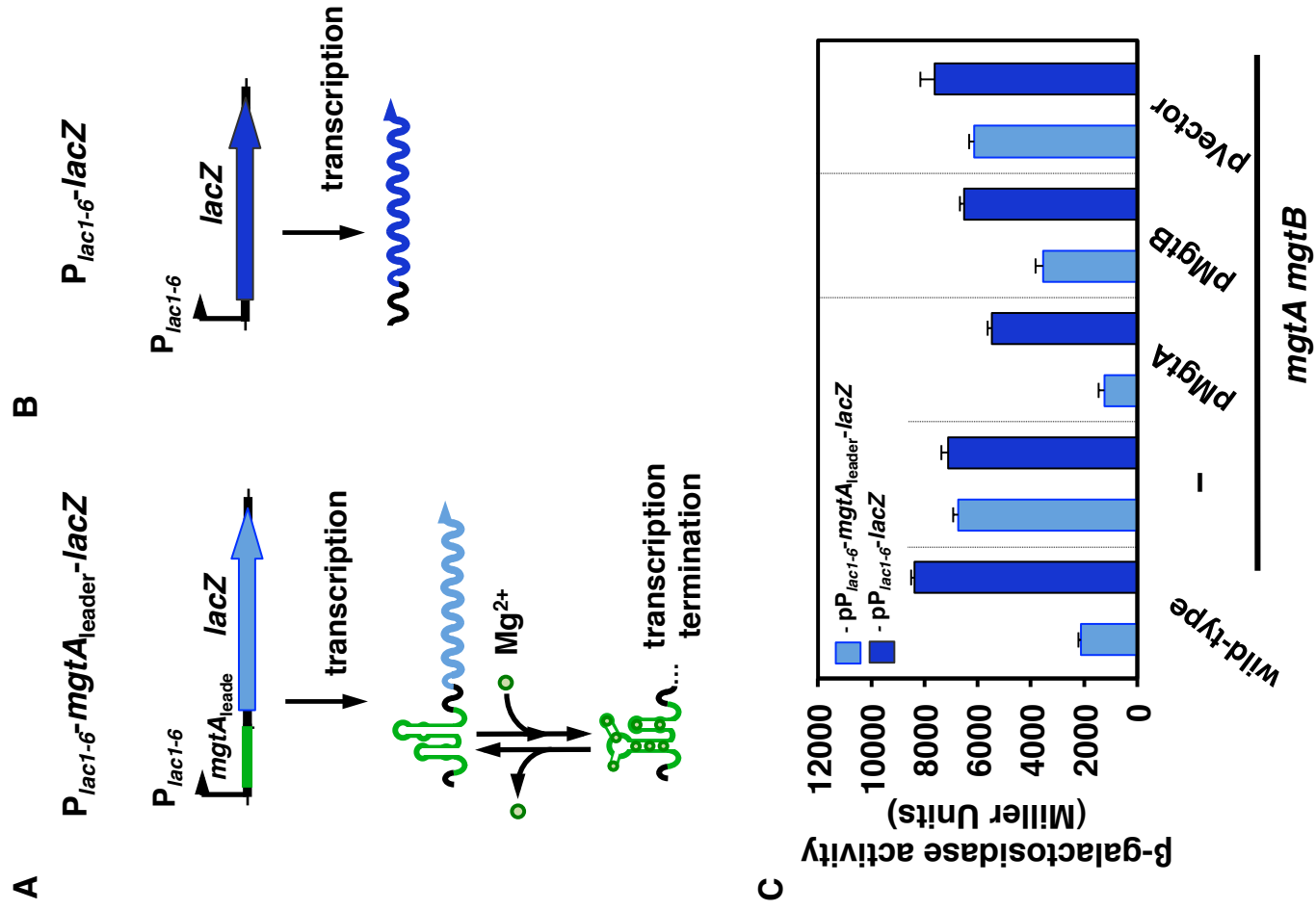


Figure S5

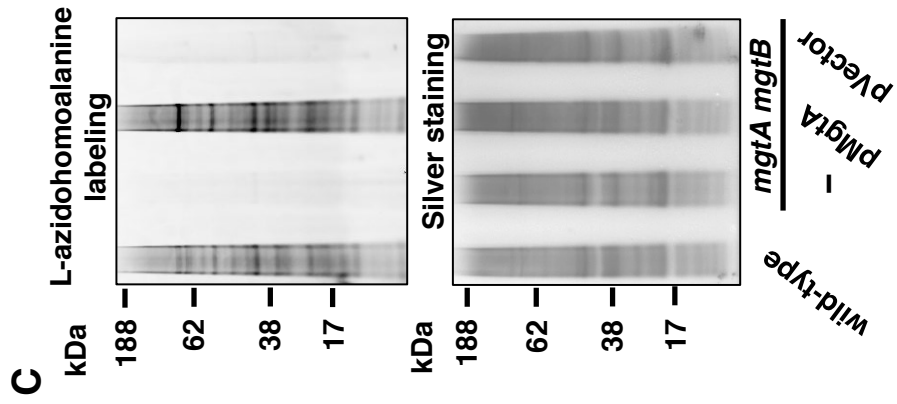
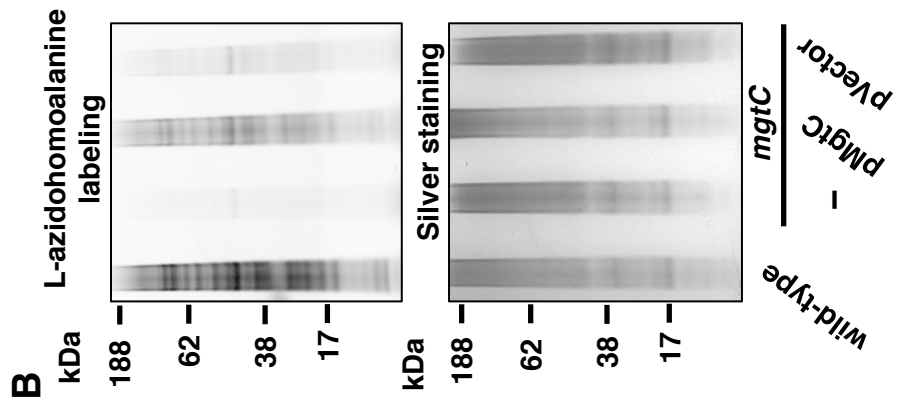
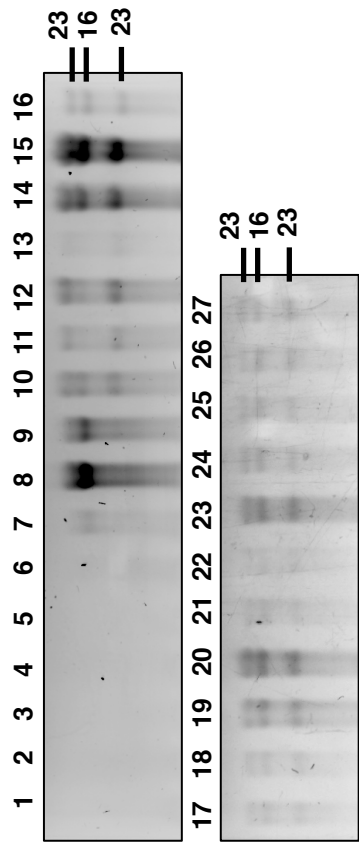
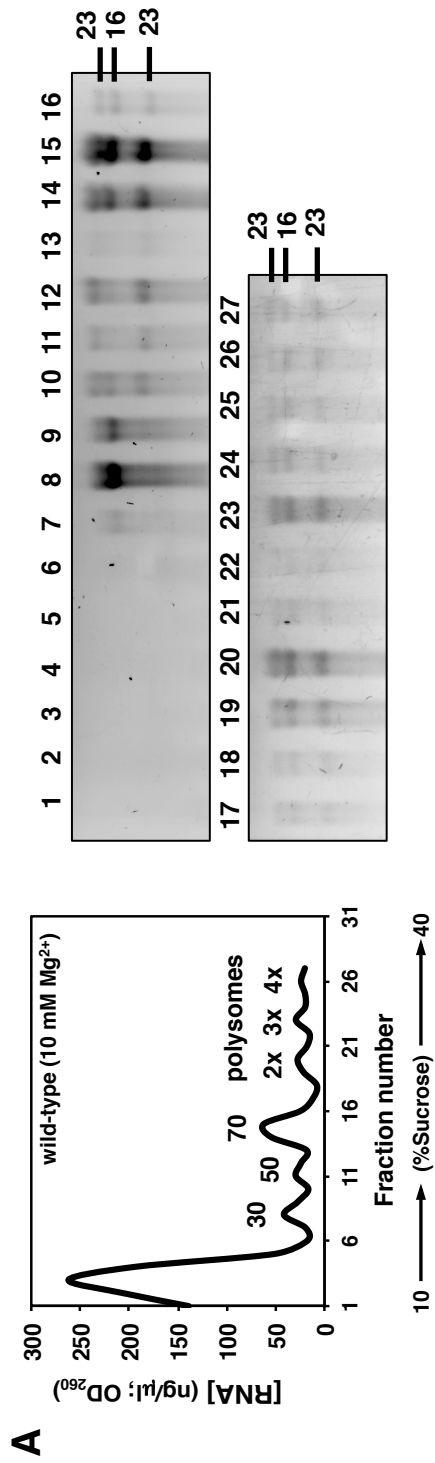


Figure S6

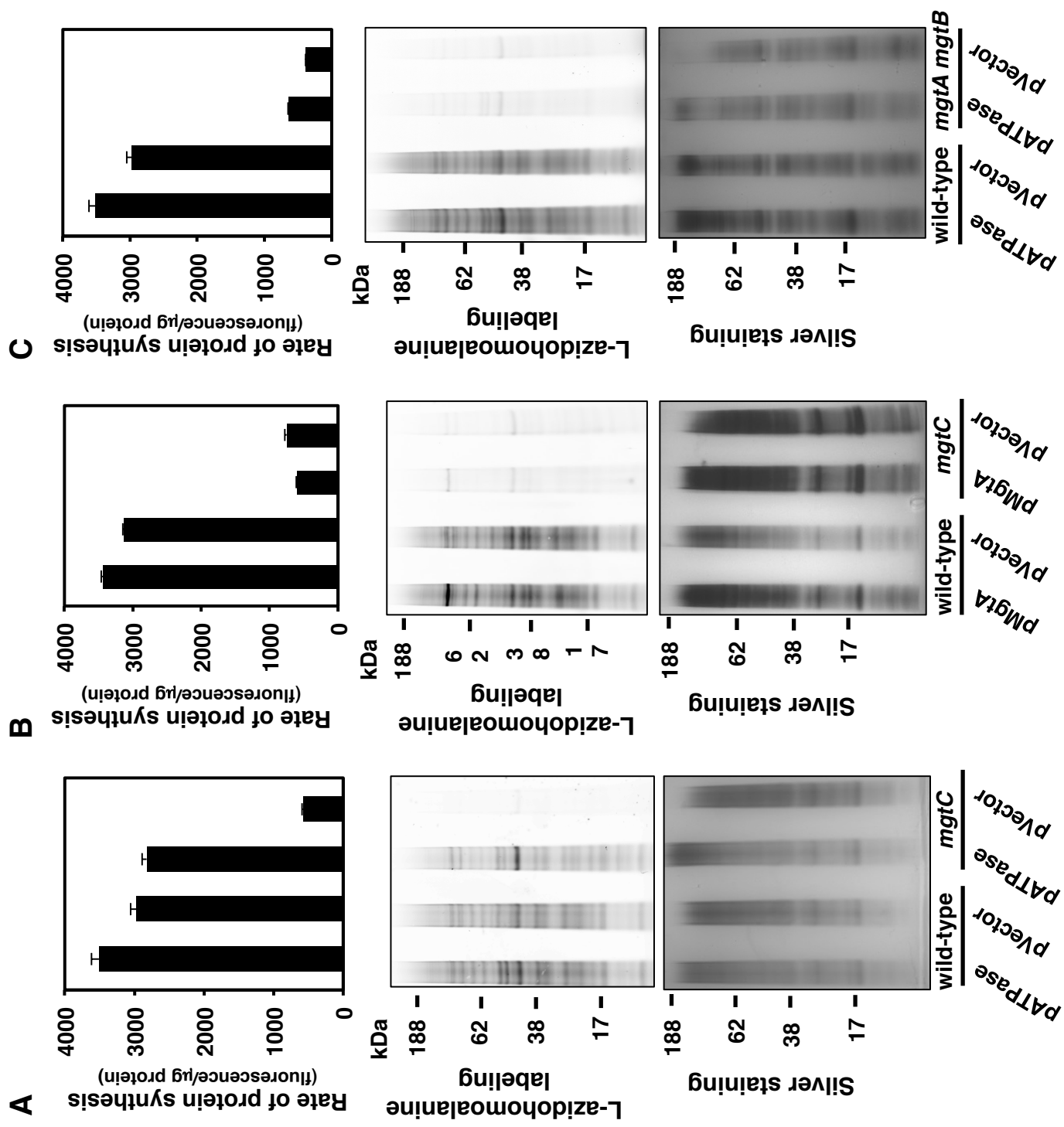


Figure S7

